# The effect of standoff distance on the electrochemical corrosion behavior of Zn-Al pseudo alloy coating by arc spray on low carbon steel in a seawater environment

S. djerourou and Y. Mebdoua

*Center for the Development of Advanced Technologies,*
*City of 20 August 1956, Baba Hassen, BP no 17, Algiers, Algeria.*

Received 4 July 2024; accepted 18 November 2024

An experimental study of Zn-Al pseudo alloy coatings prepared by twin dissimilar Zn and Al wires using the arc spray process at a different standoff distance, in order to protect low carbon steel substrates from marine corrosion has been undertaken in the present paper. The corrosion behavior of a Zn-Al pseudo alloy coating in a seawater solution collected from the Mediterranean Sea (Algerian coast) was evaluated by open circuit potential (OCP), potentiodynamic polarization, and electrochemical impedance spectroscopy (EIS) tests. The obtained results reveal that all prepared Zn-Al pseudo alloy coatings can protect the substrate, but the coating obtained at 100 mm standoff distance with 55.73% Zn and 44.27 % Al presents a better performance in corrosion protection when exposed to seawater solution compared to Zn-Al pseudo alloy coatings prepared at 120 and 140 mm standoff distances, respectively. A strong correlation is also observed between corrosion data, porosity fraction, and hardness.

*Keywords:* Twin wire arc spray; zinc-aluminum; standoff distance; corrosion; electrochemical impedance spectroscopy; potentiodynamic polarization.

DOI: https://doi.org/10.31349/RevMexFis.71.031004

## 1. Introduction

Low carbon steel is widely used in a large number of applications, including automobile frames, pipelines, ship plates, bridge beams, etc. These applications are driven by manufacturing requirements for their mechanical properties [1]. However, low carbon steel exhibits a low resistance to corrosion, and progressive deterioration of its structure leads to rust formation and consequent loss of some of its mechanical properties. Protective coating is the best method of preventing low carbon steel corrosion [2]. The most widely used metallic protective coatings are zinc, aluminum, and combinations of Zn and Al [3–8]. Al coating can protect steel for a long time because it functions as a barrier coating through the formation of a thin oxide layer (passivating film) [9, 10], but aluminum is subject to pitting corrosion [11]. Zinc coatings are widely used in industry; they provide cathodic protection, with Zn being the sacrificial anode and first corroded rather than low carbon steel [12, 13]. Therefore, Zn-Al composite coatings offer the advantage of double protection from corrosion phenomena. At present, a 85% Zn-15% Al alloy has been widely applied to the metal structure in order to enhance its resistance to corrosion [14–17]. Several authors have studied Zn-Al coatings; as an example, H. Seung Lee *et al*. [18] reported that the enhanced corrosion resistance properties of the Zn-Al pseudo alloy coating in a 3.5 wt.% NaCl solution were observed with prolonged exposure. In Ref. [19], the authors have studied the corrosion behavior of the carbon steel plates with Zn, Al and Zn-Al thermally sprayed coatings exposed to the coastal area for about 33 years; the high corrosion performance is attributed to the Zn-Al coatings. A new coating named "Zincal", produced by different combinations of Zn and Al, is deposited on low carbon steel [20] presents the best corrosion resistance in humid and salt containing environments. Recently, Zn-Al coating has provided effective corrosion protection for the S135 drill pipe steel for different Zn-Al proportions [21]. Different thermal spray processes, including high-velocity oxy-fuel, plasma, and arc thermal spray, are widely used for metal, ceramic, and plastic coating in order to improve the surface treated properties. Thermal arc spray is largely used for Zn, Al, and their alloy coatings because it offers several advantages over other coating processes, such as low cost, high spray rate, and the ability to be used on-site [22, 23]. As a result, the utilization of the process in different areas of the industry becomes ubiquitous, such as aero-turbines, automotive engines, oil and gas exploration, etc. [24, 25]. The principle of the process is to burst a direct current (DC) arc between two consumable conducting wires; the high temperature of the arc melts the wire tips, a gas flow atomizes this molten or semi molten material, and then propels the resulting droplets toward the substrate to be coated. The properties of the obtained coating depend strongly on the spray parameters [7, 26, 27]. The correlation between these parameters and coating properties is of crucial importance in order to improve the quality of the obtained coating. In this study, the authors aimed to investigate the effect of the spray parameters, namely the standoff distance (SOD), on the protective coating formed by using two dissimilar wires, Zn and Al, in order to obtain a Zn-Al pseudo alloy coating with a different percentage of zinc and aluminum deposited on a low carbon steel substrate. The electrochemical corrosion behavior of the Zn-Al pseudo alloy coating exposed to the Mediterranean seawater solution was estimated using open circuit potential (OCP), DC polarization, and electrochemical impedance spectroscopy (EIS) measurements. The porosity fraction and hardness are also measured in order to correlate with corrosion data.

## 2. Experimental procedures

### 2.1. Spray equipment and parameters

This study makes use of a twin wire arc spray gun type ARC-SPRAY 234 connected to a DC power supply (Metallization Ltd.) and two sprayed materials: (a) 01E Zinc (99.99%) 1.6 mm in diameter, and (b) 02E Aluminum (99.5%) 1.6 mm in diameter, both belonging to Metallization Ltd., in order to produce Zn-Al pseudo alloy coatings on low carbon steel XC38 disc substrates of 8 and 25 mm in thickness and diameter, respectively. The resulting coating thickness varies from 300 to 500 $\mu$m according to the standoff distance. The experimental setup was presented in our previous work [28]. The test solution used in this study was seawater collected from the Mediterranean Sea (Algerian coast). Tables I and II summarize the different spraying parameters used in this study and the sample designations, respectively.

### 2.2. Surface morphology

The microstructure of the coatings were studied by scanning electron microscopy (SEM) JEOL-3660LV model in order to measure the porosity fraction of the different samples using dot counting measuring in the cross sectional surface of the coating. Meanwhile, energy dispersive spectroscopy (EDS) is used in order to determine the percentage of elements in the coating.

TABLE I. Twin wires arc spraying parameters [28].

| Parameter | Value |
|---|---|
| Arc voltage (V) | 38 |
| Arc current (A) | 100 |
| Atomizing gas | air |
| Atomizing gas pressure (bar) | 3.8 |
| Substrate table rotation (tr/min) | 5 |
| Spray distance (mm) | 100, 120, 140 |
| Spray duration (s) | 30 |

TABLE II. Sample designations.

| Sample designations | Standoff distance |
|---|---|
| $E_0$ | Low carbon steel substrate |
| $E_1$ | 100 mm |
| $E_2$ | 120 mm |
| $E_3$ | 140 mm |

### 2.3. Hardness measurement

Hardness measurements were obtained using Vickers micro-hardness with a load of 200 g for 15 s.

### 2.4. Corrosion characterization materials

The Zn-Al pseudo alloy coatings (samples) were characterized by different techniques. The electrochemical data were derived using the Volta Lab 40 model combined with the Volta Master 4 software. The cell used is a conventional three electrode with the sample as the working electrode with 1 cm$^2$ of exposed area, a saturated calomel electrode (SCE) as a reference electrode, and a platinum plate electrode as a counter electrode. All electrochemical experiments were performed in a seawater solution at room temperature under static and aerated conditions. For open circuit potential measurements (OCP), the coatings were kept in the solution for 1 hour in order to establish the free corrosion potential ($E_{\text{corr}}$). The potentiodynamic polarization measurements were recorded by applying a potential from -1500 mV to 1000 mV with a scanning rate of 5 mV/s. The corresponding corrosion potential ($E_{\text{corr}}$), corrosion current density ($I_{\text{corr}}$), and polarization resistance ($R_p$) were extracted from the plots using the Tafel extrapolation method. The electrochemical impedance spectroscopy measurements (EIS) were carried out in the frequency range from 65 kHz to 10 MHz with respect to the open circuit potential, at a rate of 10 points per decade change in frequency. The results were fitted to get the electrical equivalent circuit (EEC).

## 3. Results and discussions

Compared to the coating prepared by cored wire, the percentage of aluminum and zinc in the pseudo alloy coating obtained by twin dissimilar Zn and Al wires using an arc spray process is unknown. For this reason, and in order to compare it to the coating prepared by conventional 85% Zn-15% Al, scanning electron microscopy (SEM) combined with energy dispersive spectrometry (EDS) analysis was performed on the cross sectional surface of the $E_1$, $E_2$, and $E_3$ samples to determine the percentage of Zn and Al. Figure 1 summarizes the obtained results as a histogram. For the $E_1$ (55.73% Zn and 44.27% Al) sample, the proportion of Zn is significant compared to that of Al; two factors seemed to account for this behavior: first, the aluminum low density (2.71 kg/m$^3$), which is approximately 2.64 times lower than the zinc density (7.135 kg/m$^3$), and second, the aluminum higher melting point (660.3 C$^\circ$) compared to zinc (419.5 C$^\circ$), which may affect the viscosity of the molten metal droplets and consequently the proportion of Zn and Al in the coatings. The situation is inverted when the standoff distance increases for $E_2$ (50.2% Zn and 49.8% Al) and $E_3$ (41.115% Zn and 50.055% Al). This may be explained by a more significant cooling of molten and semimolten Zn droplets before reaching the substrate; then they cannot contribute to coating formation.

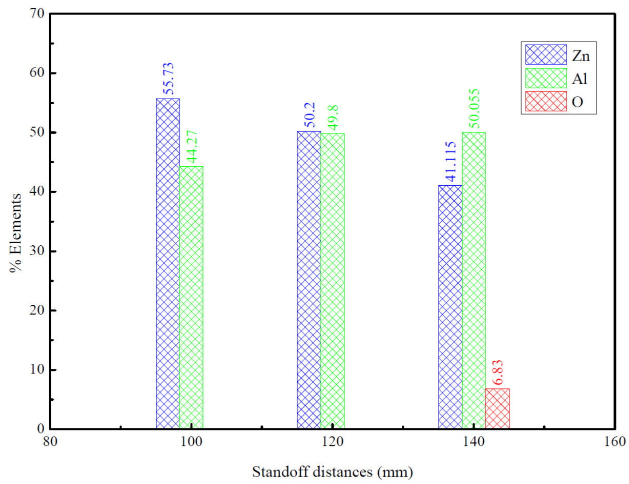


FIGURE 1. Zn and Al proportions in the cross sectional surface of the Zn-Al pseudo alloy coatings.

However, in the case of the $E_3$ sample, the presence of oxygen is caused by the high percentage of aluminum and a large standoff distance (140 mm), which gives the molten aluminum droplet enough time to be oxidized.

The first electrochemical characterization of the obtained Zn-Al pseudo alloy coatings was carried out by open circuit potential. The OCP measurement is one of the electrochemical tests used to assess and predict the corrosion performance of the coating layers. The OCP results indicate the thermodynamic tendency of the coating to electrochemical oxidation/passivation in a corrosive medium, and the objective of its measurement is to obtain the potential of the coating without influencing the electrochemical reactions on the coating surface. Following an immersion time, OCP often reaches a constant value of $E_{\text{corr}}$. However, the OCP was employed in the current investigation to estimate the corrosion potential. An evolution of the OCP for the three prepared samples at different standoff distances immersed in seawater solution is depicted in Fig. 2. We observe a decrease in the OCP of the three prepared samples, indicating that the corrosion thermodynamic tendency has increased. In regards to the $E_1$ sample, the OCP curve presents an abrupt decrease and stabilizes after 20 min of immersion time at and $E_{\text{corr}}$ of $-1.044$ V/SCE. And the OCP of the $E_2$ and $E_3$ samples exhibits a little decrease, and they stabilized after 20 min at $-1.076$ and $-1.078$ V/SCE values of the corrosion potential, respectively. The evolution of OCP between 0 and 20 min can be attributed to the destruction of a virgin aluminum oxide film formed during the spray process [5]. It is clear from the first electrochemical test (OCP) results, that the $E_1$ sample presents good corrosion protection compared to the $E_2$ and $E_2$ samples, respectively.

In order to further analyze the corrosion data, the potentiodynamic polarization measurements of low carbon steel substrate and pseudo alloy coatings corresponding to $E_1$, $E_2$ and $E_3$ samples in a seawater solution at room temperature under static and naturally aerated conditions are made, and the corresponding plots are shown in Fig. 3. The shape of the curves shows that the cathodic branch of the three samples and the substrate are identical, whereas their anodic branches differ considerably. We observe the formation of pseudopassive zones for $E_1$, $E_2$ and $E_3$, characterized by a small increase or constant value of current with an increase in potential (as shown in Fig. 3).

This phenomenon occurs when the protective layer does not cover the entire surface of the coating or when the passivating layer is metastable and reacts with the environment. This explanation confirms the presence of the protective layer as seen in the OCP data. The values of electrochemical parameters such as corrosion potential ($E_{\text{corr}}$), corrosion current density ($I_{\text{corr}}$), and polarization resistance ($R_p$) were extracted from DC polarization curves using Tafel extrapolation methods and listed in Table III.

The obtained results reveal that the substrate has a higher positive corrosion potential (-0.930 V) than that of the $E_1$, $E_2$ and $E_3$ samples. We also observe that the corrosion potential shifts toward more negative values for $E_1$ ($-1.058$ V),

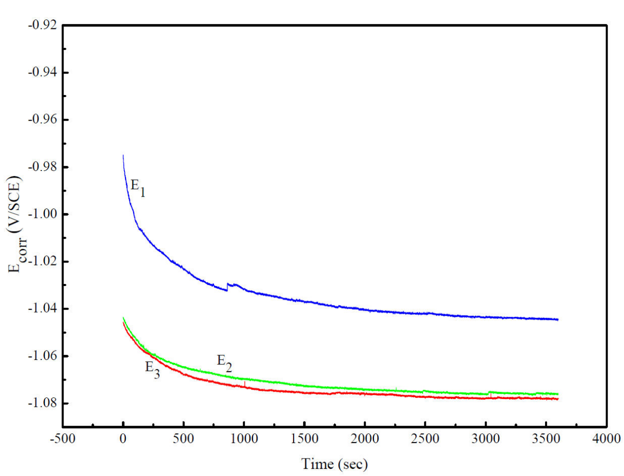


FIGURE 2. OCP Evolution of Zn-Al pseudo alloy coatings as function of immersion time in seawater solution.

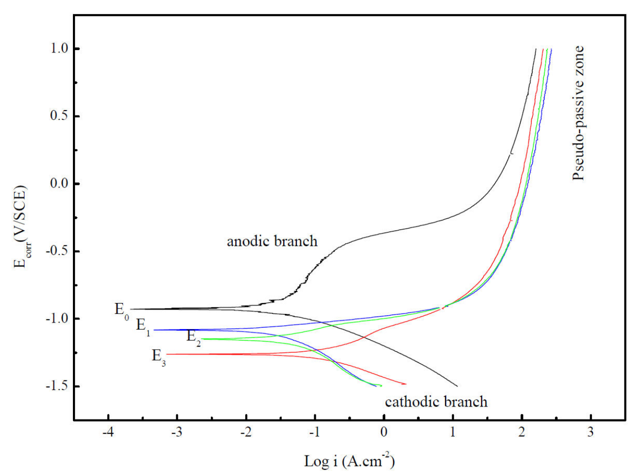


FIGURE 3. Potentiodynamic polarization curves of Zn-Al pseudo alloy coatings and low carbon steel substrate as a function of immersion time in a seawater solution.

TABLE III. Electrochemical parameters obtained from potentiodynamic polarization cureves: Corrosion potential ($E_{\text{corr}}$), corrosion current density ($I_{\text{corr}}$), polarization resistance ($R_p$).

| Sample | $E_{\text{corr}}$ (V) | $I_{\text{corr}}$ (mA.cm$^2$) | $R_p$ (ohm.cm) |
|---|---|---|---|
| $E_0$ | $-0.930$ | 6.89 | 1730 |
| $E_1$ | $-1.058$ | 6.55 | 1240 |
| $E_2$ | $-1.155$ | 10.79 | 865.42 |
| $E_3$ | $-1.265$ | 38.15 | 301.56 |

$E_2$ ($-1.155$ V) and $E_3$ ($-1.265$ V) when the SOD increases. It can be seen from these corrosion potentials that the protection of low steel substrates is made by a sacrificial anode, because this protection is more favorable when the corrosion potential is high ($E_1$). On the other hand, the corrosion current increases when the standoff distance increases; it ranges from 6.55 $\mu$A.cm$^{-2}$ for the $E_1$ sample to 10.79 $\mu$A.cm$^{-2}$ for the $E_2$ sample, and nearly six times higher for the $E_3$ sample at 38.15 $\mu$A.cm$^{-2}$. Inversely to the corrosion current, the polarization resistance decreases as follows: 1240 ohm.cm, 865.42 ohm.cm and 301.56 ohm.cm with standoff distances of 100, 120, and 140 mm, respectively. Therefore, lower corrosion current and higher polarization resistance values translate into a lower corrosion rate. The sample prepared at 100 mm presents good cathodic protection through a sacrificial anodic action and long term corrosion protection through a barrier effect. The standoff distance and the percentage of aluminum and zinc in the pseudo alloy coating have no significant influence on the shape of the anodic and cathodic branches of the potentiodynamic polarization curve, but the difference is noticeable in the value of the corrosion potential. Figure 4 presents a plot depicting the variation of the corrosion potential and hardness versus the porosity fraction for three prepared samples at different standoff distances. Two distinct rates of decline are observed in Fig. 4. This evolution can be attributed to two phenomena: the first is the solidification of the molten particles before reaching the substrate, and the second is the oxidation of the molten aluminum droplet; consequently, the coating defects increase. For the first results, we observe that the $E_1$ simple prepared at 100 mm standoff distance by a proportion of 55.73% Zn-44.27% Al presents low porosity. A strong correlation is observed between the three parameters hardness, corrosion potential, and porosity fraction when the satndoff distance varies. In accordance with the results presented above, we observe that the pseudo alloy coating obtained at 100 mm ($E_1$) standoff distance with 55.73% Zn-44.27% Al presents a small improvement in resistance to marine corrosion phenomenon ($-1.058$ V) compared to coating deposited by the same process with conventional 85% Zn-15% Al alloy ($-1.267$, $-1.235$, and $-1.112$ V) [16,17,29].

In order to gain a better understanding of the corrosion mechanism, we report in this paragraph the results obtained from electrochemical impedance spectroscopy (EIS), which allows us to represent the data in an electrical equivalent circuit and helps us to understand both the resistive and capacitive behaviors of the electrode/electrolyte interface. The measured EIS plots of various samples are depicted as Nyquist plots in Fig. 5 and as Bode plots in Fig. 6. From the first observation, it can be seen that the shapes of the EIS plots of the three samples were different, which implies that the corrosion process follows different mechanisms. The Nyquist plots show that the $E_1$ sample presents a single capacitive semicircle with a large radius at high frequencies. The radius in EIS is an important indicator to evaluate the corrosion resistance of the coating. The large radius of the semicircle means a lower corrosion rate [30]. The single capacitive semicircle indicates that the corrosion process is mainly controlled by charge transfer.

This behavior has been observed in several coating systems in which the coating is very dense [31], which is the case of the $E_1$ sample, that present a dense structure, as published in our previous research [28], and also exhibit a low

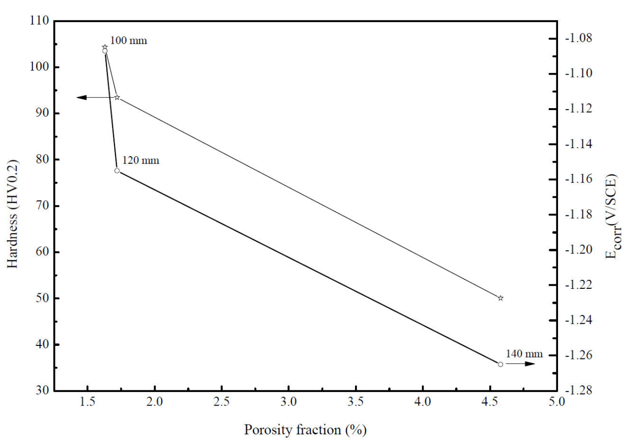


FIGURE 4. Corrosion potential and hardness variation versus porosity fraction of Zn-Al pseudo alloy coatings.

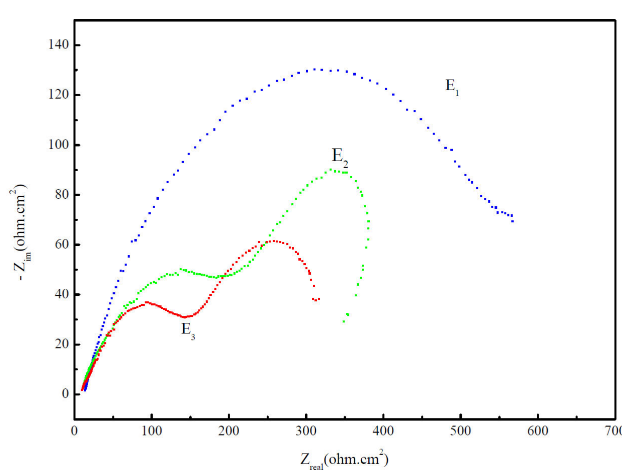


FIGURE 5. Nyquist plots for Zn-Al pseudo alloy coating.

TABLE IV. Electrochemical parameters extracted from EIS spectra using the equivalent circuit in Fig. 7.

| Sample | $Rs$ (ohm) | $R_{\text{pore}}$ (ohm) | $Rct$ (ohm) | $Q_{-c}$ in $10^{-3}$ (F.s$^{n-1}$) | $n_{Q-c}$ | $Q_{-dl}$ in $10^{-2}$ (F.s$^{n-1}$) | $n_{Q-dl}$ | $W$ (ohm.s$^{-0.5}$) |
|---|---|---|---|---|---|---|---|---|
| $E_1$ | 6.874 | 384.5 | ... | 0.409 | 0.52 | ... | ... | 15.01 |
| $E_2$ | 4.46 | 156 | 124 | 0.586 | 0.46 | 1.11 | 0.68 | ... |
| $E_3$ | 5.563 | 120.4 | 112.5 | 1.112 | 0.45 | 2.8 | 0.68 | ... |

porosity fraction. For $E_2$ and $E_3$ samples, we observe two semicircles on the Nyquist plot. The first one corresponds to the high frequency (HF) range, which is reflected in the dielectric behavior of the coating, and the second semicircle corresponds to the low frequency (LF) range, attributed to the corrosion process [32]. The first semicircle corresponding to the $E_2$ sample is larger than that of the $E_3$ sample, implying that the $E_2$ sample exhibits better resistance to the corrosion process.

The Bode plot (Fig. 6) indicates the presence of one inflection point for the $E_1$ sample. It means that the system shows a one time constant. But for $E_2$ and $E_3$, the Bode plots present two inflection points corresponding to two time constants. An examination of the various electric equivalent circuits (EEC) indicates that the best-fit of these curves (Figs. 5, 6) is given in Fig. 7, and the electrochemical parameters of the EEC are summarized in Table IV.

According to Fig. 7, we observed the presence of a basic circuit in the diagram of the EEC of the three samples. This basic circuit consists of the following elements: $Rs$ represents the solution resistance that appeared between the reference electrode and the surface of the coated sample, the dielectric property of the coating is represented by a pair of elements: $Q_{-c}$ constant phase element of the coating; and the $R_{\text{pore}}$ resistance to current flow through the pores of the coating. For the $E_1$ sample [Fig. 7a)], we observe the presence of Warburg impedance $W$ in addition to the basic circuit. Generally, Warburg impedance $W$ behavior appears when charge transfer is influenced by a semi-infinite length diffusion process occurring through the coating defects [33]. When $R_{\text{pore}}$ has an important value and the coating has a denser structure, as in the case of the $E_1$ sample [28], the ion mass transfer between the active zone and aggressive solution via a coating defect (pores) is restricted, which leads to the Warburg impedance $W$ behavior [34]. The electric equivalent circuit of the $E_2$ and $E_3$ samples [Figs. 7b) and 7c)] shows the presence of a pair of elements in parallel, the charge transfer resistance $R_{ct}$ and $Q - dl$, which is the constant-phase element of the electric double layer, in addition to the basic circuit. This EEC is proposed in Refs. [33,35] for two sub-electrochemical interfaces.

As shown in Table IV, the values of $R_{\text{pore}}$ for the three samples are inversely proportional to the standoff distance for this range of values. This result is related to the porosity rate obtained in different samples that were published in our work in Ref. [28].

When SOD decreases, the porosity rate of the same sample $E_1$ decreases, and the transfer charge of electrolyte into the coating through the pore becomes more difficult, consequently increasing the pore resistance. In the case of the $E_2$ and $E_3$ samples, the obtained results indicated that the $R_{ct}$ increases while the $Q_{-dl}$ decreases when the standoff distance decreases (Table IV). Effective corrosion resistance is associated with high $R_{ct}$ and low $Q_{-dl}$ values [36]. According to these results, we conclude that the $E_2$ sample presents good corrosion resistance compared to the $E_3$ sample.

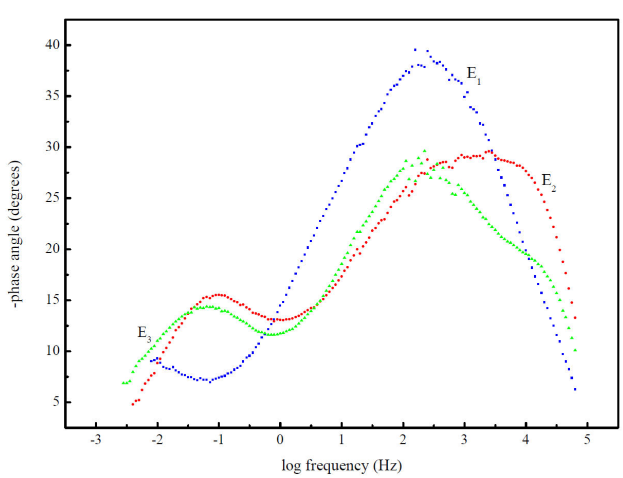


FIGURE 6. Bode plots for Zn-Al pseudo alloy coating.

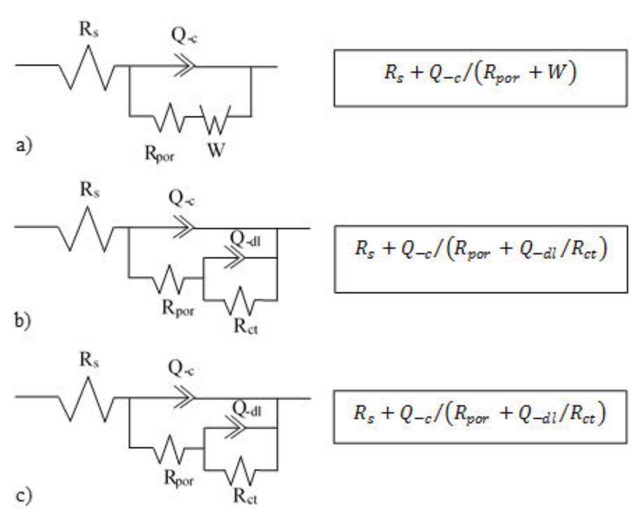


FIGURE 7. Electrical equivalent models representing the electrochemical behavior circuit of Zn-Al pseudo alloy coatings.

## 4. Conclusion

In this study, low carbon steel substrates were coated with a Zn-Al pseudo alloy using two dissimilar arc sprayed wires (Zn and Al) at different standoff distances. The Zn-Al pseudo alloy coating is used to protect low carbon steel substrates from marine corrosion. From the present investigation, the most relevant conclusions are summarized as follows:

- The percentage of zinc and aluminum in the obtained pseudo aloy coating depends on the standoff distance.
- In accordance with the corrosion test results, open circuit potential, DC polarization, and electrochemical impedance spectroscopy, the three Zn-Al pseudo alloy coatings can protect the substrate.
- A strong correlation is observed between the three parameters corrosion potential, hardness, and porosity fraction when the standoff distance is varied.
- A better performance for corrosion protection is attributed to the coating obtained at 100 mm standoff distance with 55.73% Zn-44.27% Al.
- The $E_1$ sample presents a small improvement in corrosion phenomena compared to the coating prepared with the conventional 85% Zn-15% Al alloy.

1. R. I. L. Guthrie and J. J. Jonas, Properties and selection: Irons, Steel and High. Performance Alloys, 2nd ed. (ASM International, ASM World Headquarters 9639 Kinsman Road Materials Park, OH 44073-0002, 1993), pp. 300-304.
2. Z. Chu *et al*., Corrosion mechanism of plasma-sprayed febased amorphous coatings with high corrosion resistance, *Journal of Thermal Spray Technology* **29** (2020) 1111, https://doi.org/10.1007/s11666-020-01030-9.
3. D. Varacelle *et al*., Experimental studies of twin-wire electric arc sprayed zinc/aluminum alloy coatings, *Journal of Thermal Spray Technology* **7** (1998) 513, https://doi.org/10.1361/105996398770350738.
4. M. Büteführ, Zinc-Aluminium-Coatings as Corrosion Protection for Steel, *Materials and Corrosion* **58** (2007) 721, https://doi.org/10.1002/maco.200704058.
5. D. Dzhurinskiy *et al*., Corrosion protection of light alloys using low pressure cold spray, *Journal of thermal spray technology* **21** (2012) 304, https://doi.org/10.1007/s11666-011-9729-7.
6. S.-J. Kim and Y.-B. Woo, Coating layer and corrosion protection characteristics in sea water with various thermal spray coating materials for STS304, *Surface Review and Letters* **17** (2010) 299, https://doi.org/10.1142/S0218625X10013783.
7. K.-M. Moon *et al*., Observation of the Corrosion Characteristics of Metalizing Film in Seawater Solution, *International Journal of Modern Physics B* **25** (2011) 4241, https://doi.org/10.1142/S0217979211066672.
8. S. Hong *et al*., Corrosion behavior of arc-sprayed Zn-Al coating in the presence of sulfate-reducing bacteria in seawater, *Journal of Materials Engineering and Performance* **24** (2015) 4449, https://doi.org/10.1007/s11665-015-1729-1.
9. L. Niu *et al*., A aluminum coating with chromium-free passivating film formed on AZ91D magnesium alloy, *Journal of Alloys and Compounds* **635** (2015) 11, https://doi.org/10.1016/j.jallcom.2015.02.107.
10. S. Feliu Jr *et al*., Passivating oxide film and growing characteristics of anodic coatings on aluminium alloys, *Applied Surface Science* **254** (2008) 2755, https://doi.org/10.1016/j.apsusc.2007.10.015.
11. S. F. Bonabi *et al.*, Structure and corrosion behavior of arc-sprayed Zn-Al coatings on ductile iron substrate, *Journal of Thermal Spray Technology* **27** (2018) 524, https://doi.org/10.1007/s11666-018-0694-2.
12. O. Ø. Knudsen *et al*., Experiences with thermal spray zinc duplex coatings on road bridges, *Coatings* **9** (2019) 371, https://doi.org/10.3390/coatings9060371.
13. N. M. Chavan *et al*., The corrosion behavior of cold sprayed zinc coatings on mild steel substrate, *Journal of thermal spray technology* **22** (2013) 463, https://doi.org/10.1007/s11666-013-9893-z.
14. Z. Panossian *et al*., Steel cathodic protection afforded by zinc, aluminium and zinc/aluminium alloy coatings in the atmosphere, *Surface and Coatings Technology* **190** (2005) 244, https://doi.org/10.1016/j.surfcoat.2004.04.023.
15. M. Baker *et al.*, Morphologies and corrosion properties of PVD Zn-Al coatings, *Surface and Coatings Technology* **125** (2000) 207, https://doi.org/10.1016/S0257-8972(99)00550-2.
16. B.-l. Lin, X.-Y. Lu, and L. Li, Corrosion behaviors of arc spraying single and double layer coatings in simulated Dagang soil solution, *Transactions of Nonferrous Metals Society of China* **19** (2009) 1556, https://doi.org/10.1016/S1003-6326(09)60069-8.
17. B. Lin, X. Lu, and L. Li, Electrochemical corrosion behavior of arc sprayed Zn and Zn15Al coatings in simulated salina soil and neutral meadow soil solutions, *Journal of Wuhan University of Technology-Mater. Sci. Ed.* **26** (2011) 1152, https://doi.org/10.1007/s11595-011-0380-4.
18. H.-S. Lee *et al*., Corrosion mechanism and kinetics of Al-Zn coating deposited by arc thermal spraying process in saline solution at prolong exposure periods, *Scientific reports* **9** (2019) 3399, https://doi.org/10.1038/s41598-019-39943-3.
19. H. Katayama and S. Kuroda, Long-term atmospheric corrosion properties of thermally sprayed Zn, Al and Zn-Al

coatings exposed in a coastal area, *Corrosion Science* **76** (2013) 35, https://doi.org/10.1016/j.corsci.2013.05.021.

20. S. Tailor, A. Modi, and S. Modi, Synthesis, microstructural, corrosion and antimicrobial properties of Zn and Zn-Al coatings, *Surface Engineering* **35** (2019) 736, https://doi.org/10.1080/02670844.2019.1565680.
21. D. Lv, T. Zhang, and F. Gong, Study on Properties of Cold-Sprayed Al-Zn Coating on S135 Drill Pipe Steel, *Advances in Materials Science and Engineering* **2020** (2020) 9209465, https://doi.org/10.1155/2020/9209465.
22. J. R. Davis *et al*., Handbook of thermal spray technology (ASM international, 2004).
23. C. U. Hardwicke and Y.-C. Lau, Advances in thermal spray coatings for gas turbines and energy generation: a review, *Journal of Thermal Spray Technology* **22** (2013) 564, https://doi.org/10.1007/s11666-013-9904-0.
24. D. R. Marantz and D. R. Marantz, State of the art arc spray technology, Thermal Spray Research and Applications (1990).
25. I. Hammad, Robotic Arc Spraying, *Thermal Spray Research and Applications* (1992) 651.
26. G. Jandin *et al*., Correlations between operating conditions, microstructure and mechanical properties of twin wire arc sprayed steel coatings, *Materials Science and Engineering: A* **349** (2003) 298, https://doi.org/10.1016/S0921-5093(02)00767-0.
27. I. Gedzevicius and A. V. Valiulis, Analysis of wire arc spraying process variables on coatings properties, *Journal of Materials Processing Technology* **175** (2006) 206, https://doi.org/10.1016/j.jmatprotec.2005.04.019.
28. S. Djerourou *et al*., Study of twin wire arc sprayed zinc/aluminum coating on low carbon steel substrate: application to corrosion protection, *Advanced materials research* **685** (2013) 271, https://doi.org/10.4028/www.scientific.net/AMR.685.271.
29. Q. Jiang *et al*., Electrochemical corrosion behavior of arc sprayed Al-Zn-Si-RE coatings on mild steel in 3.5% NaCl solution, *Transactions of Nonferrous Metals Society of China* **24** (2014) 2713, https://doi.org/10.1016/S1003-6326(14)63402-6.
30. T. Ishizaki, Y. Masuda, and K. Teshima, Composite film formed on magnesium alloy AZ31 by chemical conversion from molybdate/phosphate/fluorinate aqueous solution toward corrosion protection, *Surface and Coatings Technology* **217** (2013) 76, https://doi.org/10.1016/j.surfcoat.2012.11.076.
31. J. Guilemany *et al*., Influence of spraying parameters on the electrochemical behaviour of HVOF thermally sprayed stainless steel coatings in 3.4% NaCl, *Surface and Coatings Technology* **200** (2006) 3064, https://doi.org/10.1016/j.surfcoat.2005.02.116.
32. D. Yang *et al*., EIS diagnosis on the corrosion behavior of TiN coated NiTi surgical alloy, *Current Applied Physics* **5** (2005) 417, https://doi.org/10.1016/j.cap.2004.11.002.
33. C. Liu, Q. Bi, and A. Matthews, EIS comparison on corrosion performance of PVD TiN and CrN coated mild steel in 0.5 N NaCl aqueous solution, *Corrosion Science* **43** (2001) 1953, https://doi.org/10.1016/S0010-938X(00)00188-8.
34. C. Liu *et al*., An electrochemical impedance spectroscopy study of the corrosion behaviour of PVD coated steels in 0.5 N NaCl aqueous solution: Part II.: EIS interpretation of corrosion behaviour, *Corrosion science* **45** (2003) 1257, https://doi.org/10.1016/S0010-938X(02)00214-7.
35. W. Mulder *et al*., Tafel current at fractal electrodes: Connection with admittance spectra, *Journal of electroanalytical chemistry and interfacial electrochemistry* **285** (1990) 103, https://doi.org/10.1016/0022-0728(90)87113-X.
36. A. Yağan, N. Ö. Pekmez, and A. Yıldız, Corrosion inhibition by poly (N-ethylaniline) coatings of mild steel in aqueous acidic solutions, *Progress in organic coatings* **57** (2006) 314, https://doi.org/10.1016/j.porgcoat.2006.09.010.